Cerebral Plasticity After Subcortical Stroke as Revealed by Cortico-Muscular Coherence

Fei Meng, Kai-Yu Tong, *Senior Member, IEEE*, Suk-Tak Chan, Wan-Wa Wong, Ka-Him Lui, Kwok-Wing Tang, Xiaorong Gao, *Member, IEEE*, and Shangkai Gao, *Fellow, IEEE*

***Abstract*—The latency estimation of cortico-muscular coherence (CMCoh) could provide valuable information, especially for the pathological study. However, the conduction time from the central cortical rhythm to peripheral oscillations has not been explored for stroke patients. In this study one recently proposed method, maximizing coherence, was applied into the coherence analysis to estimate the latency by which the extensor carpi radialis electromyographic signals lagged behind the electroencephalographic time series with seven subcortical stroke subjects. Significantly prolonged conduction time was found in affected sides compared with the unaffected sides. The interhemispheric spatial displacement was also calculated using electrodes projection optimization and spherical surface laplacian. The results showed that the CMCoh could help investigate the cerebral reorganization after stroke.**

***Index Terms*—Cerebral plasticity, cortico-muscular coherence, stroke.**

I. Introduction

ALTHOUGH stroke often results in some degree of long-term motor impairment, most patients experience some functional recovery in the acute stage and chronic stage. It is believed that the plasticity of the central nervous system (CNS) might be one of the key factors for the recovery after stroke. The cerebral plasticity is a lifelong ability of the brain to reorganize its neural networks and pathways to adapt to changes in the environment or new tasks. Recent neuroimaging and transcranial magnetic stimulation (TMS) studies with stroke patients have showed the displacement of brain activation in the primary motor cortex (M1) on the affected side [1]–[5]. The enhanced activation in the contralesional hemisphere was also reported during the execution of motor tasks in the affected side [1], [2]. Meanwhile TMS studies also found the prolonged conduction time along the ipsilesional corticospinal pathways [6]–[8]. These functional and neurological changes were thought to be associated with the cerebral reorganization after stroke.

The coherence between the cortical rhythm and electromyographic (EMG) signals was observed during the execution of steady-state isometric contraction and phasic movement [8]. With the coherence analysis technique, the localization of the related central rhythm could be identified. The results from the studies of Gerloff *et al.* and Salenlus *et al.* suggested that the neural assembly in the M1 was the primary generator for the cortico-muscular coherence (CMCoh) [9], [10]. The β band (around 13–35 Hz) CMCoh would be related to the descending control from M1 to the motoneurons in the spinal cord [8]–[10]. The electrocorticographic (ECoG) studies showed that the most significant coherence was always found in the representation area of muscles in the precentral gyrus [11], [12]; hence the "hot-spot" location with maximum coherence could provide localization information about the central generator. Meanwhile latency from the motor cortex to the muscles, which reflected the conduction velocity of the corticospinal tract, could also be calculated through CMCoh analysis [13], [14]. Furthermore, the CMCoh has good reproducibility [15]. Therefore, the CMCoh was an alternative way to investigate the properties of the motor system in normal as well as pathological conditions [16]–[18].

The first CMCoh study with stroke patients was conducted by Mima *et al.* [16]. They observed a significant difference in the coherence value between unaffected and affected sides. The shifted locations of the coherence peak in the affected side were also reported. However, the localization of the most significant coherence could not be shown in their study, which might possibly be due to the low density electroencephalographic (EEG) recording using 56 channels. In the current study we adopted a high resolution EEG recording (128 channels) to help provide more information toward a better understanding of the plasticity after stroke. Electrode projection optimization (EPO) and spherical surface laplacian transformation were used to identify the location of the "hot spot" that corresponded to the peak coherence. In addition, the conduction time from the motor cortex to the muscles was calculated using the maximizing coherence technique in order to provide additional information for comprehension about the brain reorganization [13].

II. Methods

A. Subjects

Persons with chronic stroke (more than 12 months after onset of stroke) were invited to join this study. Subjects were selected

Manuscript received November 28, 2007; revised May 07, 2008; accepted July 06, 2008. First published September 19, 2008; current version published July 06, 2009. This work was supported by the research funding of Hong Kong Polytechnic University (A-PA7L) and the key project of Beijing Natural Science Foundation (3051001).

F. Meng is with the Department of Biomedical Engineering, Tsinghua University, Beijing 100084, China and also with the Department of Health Technology and Informatics, Hong Kong Polytechnic University, Kowloon, Hong Kong, China (e-mail: mf99@mails.tsinghua.edu.cn).

K.-Y. Tong, S.-T. Chan, W.-W. Wong, and K.-H. Lui are with the Department of Health Technology and Informatics, Hong Kong Polytechnic University, Kowloon, Hong Kong, China (e-mail: k.y.tong@polyu.edu.hk; htphoebe@inet.polyu.edu.hk; 07900188r@polyu.edu.hk; 05136684d@polyu.edu.hk).

K.-W. Tang is with the Department of Diagnostic Radiology and Imaging, Queen Elizabeth Hospital, Hong Kong, China (e-mail: tkwz01@hotmail.com).

X. Gao and S. Gao are with the Department of Biomedical Engineering, Tsinghua University, Beijing 100084, China (e-mail: gxr-dea@tsinghua.edu.cn; gsk-dea@tsinghua.edu.cn).

Digital Object Identifier 10.1109/TNSRE.2008.2006209

TABLE I
CHARACTERISTIC OF THE STROKE PATIENTS

Case	Age	Gender	Affected side	Location of lesion	Time since stroke (months)	Fugl-Meyer assessment
1	23	M	R	Region of left basal ganglia and inferior temporal lobe	34	26
2	61	M	R	Region of left basal ganglia	38	25
3	48	F	L	Region of right basal ganglia	60	30
4	56	M	L	Region of right Basal ganglia	39	35
5	62	M	R	Region of left basal ganglia	132	25
6	50	M	L	Region of right basal ganglia	24	19
7	55	M	R	Region of left basal ganglia	72	37

F = female; M = male; R = right side paresis; L = left side paresis.

based on the following criteria: 1) the presence of unilateral hemiparesis after a single stroke event; 2) subcortical lesions with intact sensorimotor cortex; 3) modified Ashworth scale (MAS) < 2 for affected wrist; 4) age between 20 and 65. The upper limitation of age was intended to minimize the chance of the subject having difficulty concentrating during the whole experiment. Each subject's experiment lasted about 3 h. The exclusion criteria included uncontrolled medical problems, history of epilepsy and serious cognitive deficits that would limit the subject's ability to give informed consent and perform the tasks.

Seven subjects were recruited (six males and one female) and they were right handed according to the Edinburgh inventory [19]. They suffered from first ever stroke resulting in a unilateral hemiparesis. The T2-weighted MRI imaging was conducted to identify the locations of lesion with a 1.5-T scanner (Magnetom Vision, Siemens). All the subjects had lesion at the left or right region of the basal ganglia. In addition, subject 1 had extra impairment at the left inferior temporal lobe. The upper extremity portions of the Fugl–Meyer assessment (FMA) [20] were conducted and the basic characteristics of these subjects are listed in Table I. They gave informed consent and this study was approved by the ethics committees of the Hong Kong Polytechnic University and the Queen Elizabeth Hospital.

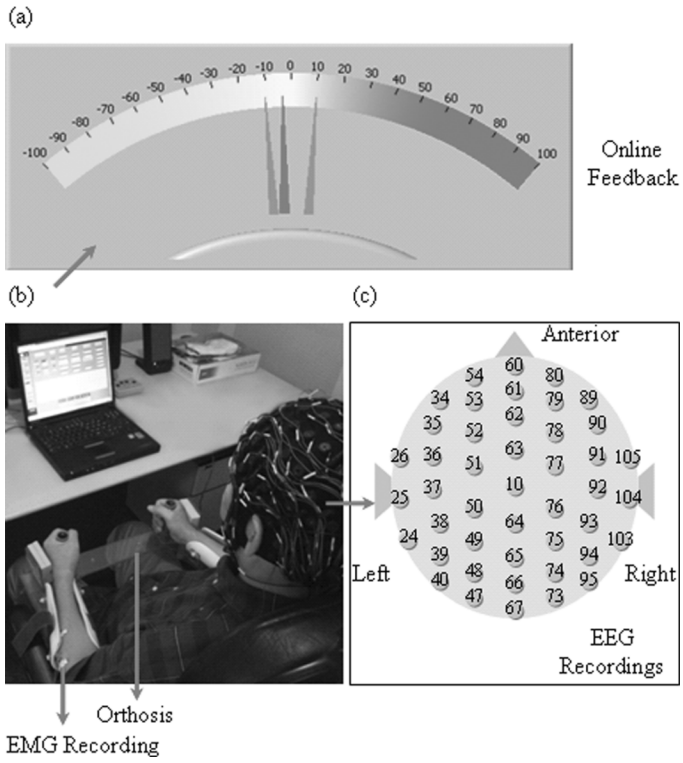

Fig. 1. Orthosis design and the EMG amplitude online control with feedback. (a) User interface for EMG amplitude online feedback control. Two gray indicators marked the acceptable $\pm 10\%$ level. (b) Demonstration of the experimental setup. (c) Top view of the 128-channel quick-cap. Subset of the electrodes was shown to indicate the electrode locations in the frontal and parietal areas.

B. Experimental Paradigm

A plastic orthosis was designed to support both the unaffected and affected arms to standardize the experimental condition. The subject was seated in a chair and the forearms were placed horizontally in the orthosis with elbow angle at 120° for both sides (180° is full extension). In the orthosis, the forearms could be positioned with straps to fix their location and also the two handles for the hands. The distance between the handles was 280 mm [Fig. 1(b)].

The EMG signals were recorded with surface electrodes from extensor carpi radialis (ECR) muscles on both the unaffected and affected side. First, the subject was instructed to execute a wrist extension of the unaffected side with maximum voluntary contraction for 5 s. The average of the absolute EMG amplitude in this duration was adopted as the maximum EMG amplitude, denoted by $\mathrm{EMG_{max}}$. As a percentage more than 50% of $\mathrm{EMG_{max}}$ could quickly lead to muscle fatigue in sustaining contraction tasks in our preliminary study, the 40% of $\mathrm{EMG_{max}}$ was selected as the control target. After the measurement of $\mathrm{EMG_{max}}$, six repetitive trials were conducted with 1 min intermittent break. The task of the subject in each trial was to contract the wrist extensor with the proper force level with real-time feedback on a 14-in computer screen, and the error between the target and measured EMG signals was calculated online according to the following equation:

$$\mathrm{Err}\% = \frac{\mathrm{EMG_{avg}} - 0.4 \times \mathrm{EMG_{max}}}{0.4 \times \mathrm{EMG_{max}}} \times 100\% \qquad (1)$$

where $\mathrm{EMG_{avg}}$ was the average of absolute EMG amplitude in the previous 2-s window and $\mathrm{Err}\%$ was fedback to the subject through a 14-in computer screen which was placed 1 m in front of the subject (Fig. 1). The ideal control corresponded to the zero value of the feedback error, and the fluctuation of the error

was instructed to be better kept within $\pm 10\%$. Totally, six trials with feedback control were conducted for the unaffected side and each trial lasted for 40 s. Then the subject experienced the measurement of $\mathrm{EMG}_{\max}$ and another six 40-s feedback trials for the affected side.

It has been documented that the cortico-muscular coherence increases after muscle fatigue [21]. Therefore, the mean power frequency (MPF) of EMG signal was calculated offline and any data with reduction of MPF above 10% will be recognized as fatigue. Meanwhile, the intermittent break was 2 min for affected trials to minimize the effect of fatigue, and no fatigue was detected from any of the subjects during the trials.

EEG and EMG activities were acquired using a Neuroscan SynAmp^2 and Scan version 4.3 (Neuroscan, Neuroscan Inc.) in an electrically shielded experimental room. High-resolution EEG signals were recorded using a Quick-Cap (Neuroscan, Neuroscan Inc.) equipped with 128 channels with linked reference electrodes on the left and right mastoid. The electrodes in the frontal and parietal area were displayed in Fig. 1(c) to indicate the location of the channels in the sensorimotor area. Surface EMG was recorded from the left and right ECR muscles simultaneously. The EEG and EMG signals were digitalized at a sampling rate of 1000 Hz. The recording bandwidth was set from dc to 200 Hz for EEG and 1Hz for EMG, respectively. All the electrode impedances were kept below 5 kΩ. After the experiment, the positions of EEG electrodes and three anatomic landmarkers: nasion, left preauricular point (PAL), and right preauricular point (PAR) were digitalized using a digitization device (Polhemus Fastrak and 3DspaceDX software, Neuroscan Inc.).

C. Coherence Analysis

The data at the beginning and end of the contraction was discarded for extracting the data with better stability for both EEG and EMG signals. A subset of the 128 EEG electrodes located around bilateral ears and at the posterior edge of the electrical cap was also rejected due to possible instable contact, and 96 electrodes were left for further processing. The spherical spline laplacian was employed to enhance the underlying cortical rhythm related to cortico-muscular coherence. The digitization device adopted the midpoint of the line segment PAL-PAR as the origin of the coordinate system. We denoted this origin by O, and the Cartesian coordinates were (x_o, y_o, z_o). Moreover, (x_n, y_n, z_n) represented the coordinates of the EEG electrodes in the same coordinate system $(n = 1, 2, \ldots, 96)$. The following coordinate transformation was applied to calculate radius r' and the optimized coordinate system with new origin O' to minimize the error of spherical assumption of the head geometry (Fig. 2).

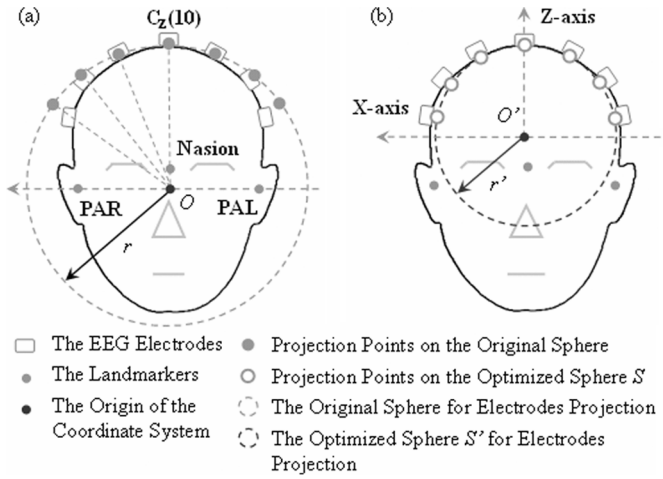

Fig. 2. Optimization of EEG electrodes projection. (a) Projection demonstration in the original coordinate system and sphere. (b) Projection onto the optimized sphere after coordinates transformation.

Step 1) (x axis Direction Identification): The x axis direction of the Cartesian coordinate system after transformation paralleled the line passing through the PAL and PAR.

Step 2) (y-z Plane Recognition): As the electrical cap was worn in a way that the central electrode (index 10, corresponded to the C_z electrode in the 64-channel system) was located at the midpoint of the nasion-inion and PAL-PAR line along the scalp, the y-z plane of the transformed coordinate system was perpendicular to the x axis direction and passed through the electrode index 10.

Step 3) (O' and r' Identification): We supposed that the coordinates of transformed origin O' were (x'_o, y'_o, z'_o) in the original coordinate system. And (x'_n, y'_n, z'_n) denoted the projection point coordinates of the EEG electrodes on the sphere centered at O' with radius $r'(n = 1, 2, \ldots, 96)$. The optimal O' and r' could be identified by solving the following optimization problem:

$$\min \left\{ \sum_{n=1}^{96} (x_n - x'_n)^2 + (y_n - y'_n)^2 + (z_n - z'_n)^2 \right\}$$
$$\text{s.t.} \quad x'_0 = x_{10}. \tag{2}$$

The x'_n, y'_n, and z'_n could be expressed as the functions of x'_o, y'_o, z'_o, and r'. These parameters could be optimized using the Nelder–Mead algorithm with initial conditions that $y'_o = 0$, $z'_o = 0$, and $r' = r$ (r denoted the distance from O to PAL or PAR).

Step 4) (x, y, and z axis Identification): The z axis was defined as the line through O' and electrode 10. The x axis was perpendicular to the y-z plane and passed through O'. The y axis was specified as the line perpendicular to the x-z plane. The origin of the coordinate system was moved to O'.

The optimal projection sphere S could be identified as the sphere centered at O' with radius r' after the transformation and optimization process. The algorithm above was named electrodes projection optimization (EPO). The projection points of the EEG electrodes on the sphere were used for the spherical Laplacian to deblur the low spatial frequency noise like background brain waves and possible contaminated EMG activities [22], [23]. The laplacian transformation could also sharpen the underlying cortical rhythm related to the task. Afterwards the spatial filtered brain signal and rectified EMG signal were segmented into nonoverlapping 1024-ms epochs. The coherence

spectrum was calculated with a fast Fourier transform algorithm, according to the following equation:

$$C(\omega) = \frac{|f_{\mathrm{xy}}(\omega)|^2}{f_{\mathrm{xx}}(\omega) \cdot f_{\mathrm{yy}}(\omega)}. \tag{3}$$

where $f_{\mathrm{xx}}(\omega)$, $f_{\mathrm{yy}}(\omega)$, and $f_{\mathrm{xy}}(\omega)$ represented the auto-spectrum and cross spectrum of selected EEG signal and EMG signal. The estimated auto-spectrum and cross spectrum on data segments were used to calculate the coherence spectrum in our analysis. The coherence calculated with (3) was the function of frequency ω. The frequency band of interest in the current study ranged from 5 to 45 Hz, which covered most of the scalp EEG spectrum. The significance of such coherence was determined with the following equation [24]:

$$\mathrm{CL}_{(\alpha\%)} = 1 - \left(1 - \frac{\alpha}{100}\right)^{\frac{1}{(N-1)}} \tag{4}$$

where α was the significance level (α was 95 in our study and corresponded to p value 0.05), N was the number of data segments, and CL represented the coherence confidential limit above which we had a significant coherence. The term "peak coherence" was utilized in this paper to describe the highest significant coherence across all EEG *projection points* in the frequency band of interest. The peak coherences of the unaffected and affected side for each subject were analyzed in this study. The routines within EEGLab toolbox have been applied to generate the topographical distribution of coherence on the scalp [25].

D. Interhemisphere Asymmetries of the Maximum Coherence

The highest significant coherence was only found at the electrode in the representation area of M1 corresponding to the contracted muscle in the ECoG based cortico-muscular coherence studies [11], [12]. The M1 related displacement after stroke has been documented in studies with fMRI, PET, and TMS [1]–[5], therefore the highest significant coherence localization possibly provided a rough estimation of the representation area shift after brain reorganization. The previous studies demonstrated that spherical laplacian could improve the spatial resolution of EEG potential distributions [22], [23]. The surface laplacian estimator reflected the continuous distribution of the current sources on the scalp. In this study, the "maximum coherence" was defined as the highest significant coherence across the *scalp* and the following method was used to identify the location of maximum coherence.

After projecting the EEG electrodes onto the optimized sphere S, the peak coherence between the scalp current and the rectified EMG signal was firstly identified across all the projection points. Then a 15×15 grid with 1 mm $\times$ 1 mm intermittent distance (x and y direction) centered at the projection point with peak coherence was specified on the sphere S. The scalp current at each node of the grid was computed with spherical Laplacian. The localization of the maximum coherence was identified as the coordinates of the node with highest significant coherence. The medial–lateral and anterior–posterior interhemisphere differences of the peak coherence localization were calculated for each subject. The positive direction of the interhemisphere differences was defined as the medial and posterior shift of the affected side compared to the unaffected side.

E. EEG-EMG Latency Analysis

Part of the EEG data and corresponding EMG time series were discarded before the latency estimation according to the following method: the autocorrelation function of each segment was calculated and the de-correlation time at which autocorrelation function falls to e^{-1} was identified [26]. Higher decorrelation time would be obtained on the nonstationary data segments due to muscle activity or other factors. Therefore, 50% of segments with higher decorrelation time were discarded empirically according to [13] and all the latency estimations were based on the data segments left.

There were several methods to estimate the delay between cortical rhythm and muscle activity [13], [14]. The maximizing coherence method was proven to be effective for latency estimation in narrow band [13]. As the delay δ between two coherent time series caused a reduction in the estimated coherence, the maximum coherence could be expected by artificially shifting the lagged signal backward with δ time points.

Let $C(\omega/\tau = 0)$ denote the coherence spectrum between original EEG and EMG time series without time shifting. We supposed that ω_0 was the corresponding frequency of the highest significant coherence between two time series, therefore, we had $C(\omega_0/\tau = 0)$ as the peak coherence value. We shifted the EMG signal backward with lag τ by keeping the EEG time series as the reference and considered coherence at ω_0 as a function of $\tau : C(\omega_0/\tau)$. The coherence will reach a maximum value $C(\omega_0/\tau = \delta)$ at the lag $\tau = \delta$.

Surrogate analysis was used to estimate the significance level of the latency estimation [13]. The surrogate of unshifted EEG time series was generated by shuffling the original segments sequence. The delayed coherence $C(\omega_0/\tau = \delta)^{\mathrm{surr}}$ was computed on surrogate EEG and shifting EMG time series. The null hypothesis was that $C(\omega_0/\tau = \delta)$ obtained was due to spurious correlations. We calculated the significance of difference CL (τ) between the $C(\omega_0/\tau)^{\mathrm{surr}}$ and $C(\omega_0/\tau)$ where

$$\mathrm{CL}(\tau) = \frac{|C(\omega_0/\tau) - \langle C(\omega_0/\tau)^{\mathrm{surr}} \rangle|}{\sigma[C(\omega_0/\tau)^{\mathrm{surr}}]} \tag{5}$$

in which $\langle\rangle$ indicated the average over realizations of surrogate and $\sigma()$ ndicated the standard deviation. Any value of CL $(\tau) > 2$ indicated that the coherence obtained was not due to spurious correlations and gave the significance level $P < 0.05$ [27].

Practically the latency δ was identified by searching for the maximum of coherence on $C'(\omega_0/\tau) = C(\omega_0/\tau) - \langle C(\omega_0/\tau)^{\mathrm{surr}} \rangle$ instead of the original $C(\omega_0/\tau)$ as we wanted to exclude the possible contribution of occasional correlation between two time series to the latency estimation. We generated different numbers of surrogates from $N = 10$–500 with data from both the affected and unaffected side for each subject. The process of synthesis was repeated 1000 times for each surrogate number N and we obtained the estimated latencies array $\boldsymbol{\delta}_N$ in each condition, where δ_N had the dimension of 1000×1. The

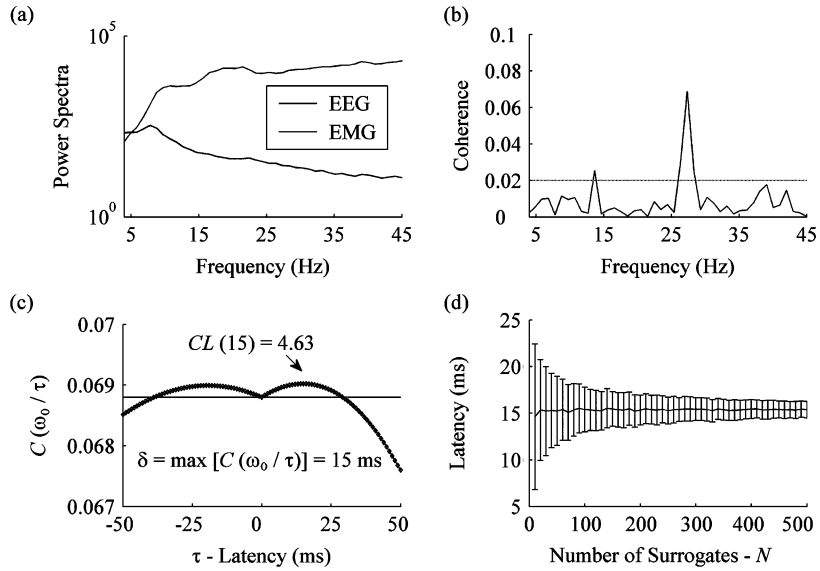

Fig. 3. Coherence and latency analysis of the unaffected task of subject 6. (a) Power spectra of channel 37 of EEG signals (gray line) and EMG signal from right ECR muscle (black line). Peak coherence was observed between these two time series among all EEG channels. Note that the power spectra were shifted for clarity. (b) Coherence between channel 37 and the EMG signal from the right ECR muscle. Maximum coherence was found at frequency 27.34 Hz. Dotted line represents the confidence level ($P < 0.05$). (c) Coherence curve observed when one of the time series was shifted while keeping another constant. The half of curve with negative latency was calculated by shifting the EEG signal backward while keeping the EMG signal constant. (d) Mean and standard derivation of $\boldsymbol{\delta}_N$ while N denotes the number of surrogates for calculating the $\langle(\omega_0\tau)^{\mathrm{surr}}\rangle$.

TABLE II
RESULTS OF THE PEAK COHERENCE, ITS CORRESPONDING FREQUENCY AND THE ESTIMATED LATENCY FROM EEG TO EMG OF ALL SUBJECTS

Case	Unaffected side			Affected side		
	Peak Coherence	Corresponding Frequency (Hz)	Latency (EEG-EMG) millisecond	Peak Coherence	Corresponding Frequency (Hz)	Latency (EEG-EMG) millisecond
1	0.1008	28.32	17.82	0.0538	24.41	20.30
2	0.1834	22.46	21.85	0.0387	31.25	27.31
3	0.0921	31.25	20.06	0.0607	16.60	18.29
4	0.0638	17.58	17.18	0.0311	35.16	24.75
5	0.0557	32.23	20.08	0.0321	20.51	24.42
6	0.0688	27.34	15.42	0.0378	27.34	20.90
7	0.1222	11.72	20.30	0.0404	28.32	26.13
mean	0.0981	24.41	18.96	0.0421	26.23	23.16
SD	0.0442	7.56	2.22	0.0111	6.32	3.35

fluctuation of the single estimation of latency $\boldsymbol{\delta}$ was obvious even when N was large [Fig. 3(d)]. Although the standard deviation of latency estimation was sensitive to the number of surrogates to use, the mean latencies $\langle\boldsymbol{\delta}_N\rangle$ from different N were rather stable. This simulation indicated that the latency $\boldsymbol{\delta}$ calculated from one realization of surrogates synthesis possibly led to the improper estimation with large deviation and encouraged us to adopt $\langle\boldsymbol{\delta}_N\rangle$ as the result of latency estimation. Therefore, we repeated the surrogate synthesis 1000 times with $N = 300$ for each subject and the results of $\langle\boldsymbol{\delta}_{300}\rangle$ were reported as the latency estimation.

III. RESULTS

For each subject 150 artifact-free segments from unaffected and affected tasks were selected for data analysis. The peak coherence and the corresponding frequency of each subject have been identified for both the affected and unaffected tasks. The latency between the EEG and EMG time series was calculated with the maximizing coherence method. The significance of such latency estimation: $\mathrm{CL}(\tau)$ was computed for all the latency estimation at delay δ based on (5). As the surrogate synthesis was repeated 1000 times for constructing the latency estimation array $\langle\boldsymbol{\delta}_{300}\rangle$, we calculated the significance $\mathrm{CL}(\tau)$ for each synthesis and constructed the significance array $\mathbf{CL}(\tau)$. The confidence level of the latency estimation was identified by the mean of the significance array. All the latencies reported here were significant ($\langle\mathbf{CL}(\tau)\rangle > 2$) and the results have been summarized in Table II.

After identifying the electrode with the highest significant coherence for both sides, the interhemisphere localization difference of the peak coherence was calculated using spherical spline Laplacian. The interside asymmetries were showed in Table III.

The mean peak coherence was 0.0981 ± 0.0442 and 0.0421 ± 0.0111 for the unaffected and affected sides, respectively (mean $\pm$ SD). The peak coherence value was statistically different between the unaffected and affected sides using paired *t*-test

TABLE III
INTERHEMISPHERE DIFFERENCE OF THE MAXIMUM COHERENCE LOCALIZATION

Case	ML (millimeter) Affected vs unaffected side	AP (millimeter) Affected vs unaffected side	Description of the shift
1	+25	+3	medial;
2	+9	+3	medial;
3	+18	+18	medial; anterior;
4	+12	+12	medial; anterior;
5	-3	-15	posterior;
6	+18	-34	medial; posterior;
7	+22	+3	medial;

ML, AP: Medial-lateral and anterior-posterior interhemisphere difference in the maximum coherence localization. The medial-lateral shift was defined as positive if the maximum location of the affected side was more medial than the one of the unaffected side, and a more posterior shift in the affected side was defined as positive in the anterior-posterior direction.

$(P = 0.0146)$. The topographic map of coherence showed the highest significant coherence in the frontocentral area of the contralateral side to the task for all the subjects, corresponding to the anatomical primary motor/sensory cortex (M1/S1). The peak coherence in the affected side task had medial shift for all subjects than their unaffected side except subject 5 (Fig. 4). Anterior shift of peak coherence of affected task could be observed in subject 3 and 4, and posterior shift was found in subject 5 and 6 (see Table III). As equivalent experimental conditions were applied to both the affected and unaffected tasks, the lesion by stroke and the following reorganization possibly resulted in the significant changes in latency.

The process of latency estimation was showed in Fig. 3. After identifying the frequency corresponding to the peak coherence [Fig. 3(b)], the time lag was computed with maximizing coherence on stationary parts of the relative electromyographic oscillation and central cortical rhythm [Fig. 3(c)]. The mean latency by which EMG signal lagged behind EEG time series was 18.96 ± 2.22 ms and 23.16 ± 3.35 ms for the unaffected and affected sides, respectively (mean $\pm$ SD). Paired *t*-test showed that the latencies of the unaffected group were significantly shorter than the latencies of the affected group $(P = 0.0108)$.

IV. DISCUSSION

A. Prolonged Conduction Time in the Affected Side

Phase coupling is both necessary and sufficient to yield nonzero coherence between two time series; therefore, CMCoh reflects the phase synchronization between central rhythm and electromyographic activities. As the CMCoh possibly represents the descending control via the corticospinal tract, the conduction time from the motor cortex to the muscles could be calculated using phase spectra analysis [28], [29]. And results comparable to the ones from TMS studies are expected. However, previous CMCoh studies showed divergent conduction time between the cortical rhythm and peripheral oscillations. Brown *et al.* reported a very short conduction time ($\sim$4 ms) between the motor cortex and wrist extensor muscles [28], and Mima *et al.* showed a shorter latency (14.3 and 15.9 ms separately) for abductor pollicis brevis (APB) muscles [29], [30], while Gerloff *et al.* found a rather fast conduction time ($\sim$9 ms) for M. extensor digitorum [9]. It remains under debate what factors contributed to such latency controversy. The computation of the coherence and latency were both based on the stationary assumption of the recorded EEG or MEG and EMG time series. However, the hypothesis of stationarity could be easily rejected due to contaminated artifacts like the offset drift, blinking, and muscle contraction, etc., which results in a low signal noise ratio of the brain signals. Consequently, the accuracy of the latency estimation might be improved by neglecting the segments of EEG or MEG time series with less stationarity. In the light of such conjecture, Govindan *et al.* successfully applied a method of maximizing coherence to the calculation of lag between motor cortex and muscles [13]. Part of the EEG and EMG signals with higher decorrelation time were excluded from the computation of conduction time, and the latencies for wrist extensor muscles were in keeping with a direct transmission through fast pyramidal pathways. In the MEG study by Gross *et al.*, the delays were estimated in the time window with the strongest synchronization, and comparable conduction times with TMS studies were reported for four muscle groups from upper limbs as well as lower limbs [14]. These two studies showed evidences that the partly satisfied assumption of stationarity could be an important factor for the controversy about latency estimation. Hence, the method of maximizing coherence was adopted in the current study.

The major finding of this work was the significantly prolonged conduction time between the motor cortex and ECR muscles in the affected side (see Table II). The delays were 18.96 ms for the unaffected side and 23.16 ms for the affected side, and the difference of mean latencies was about 4 ms. In the CMCoh study by Salenius *et al.*, the delays from the central rhythm to four muscle groups (biceps brachii, extensor indicis proprius, first dorsal interosseus, and flexor hallucis brevis) was investigated with right-handed normal subjects [10]. The results showed that the specific muscles from the left and right side had similar latencies, which implied that the latency differences in the current study were independent of the handiness. The mean conduction time for ECR muscles in the unaffected side was similar to ones measured with TMS ($\sim$17 ms) [31]. Therefore, the prolonged conduction time from the lesional hemisphere to the affected muscle possibly resulted from the factor of cerebral damage and succeeding brain reorganization. Indeed, Byrnes *et al.* reported as much as 5 ms difference of latency for motor evoked potential (MEP) between the affected and healthy side for well recovered stroke patients [4], and Pennisi *et al.* found significantly increased central motor conduction time (CMCT) for the lesional hemisphere [7]. Furthermore, Stinear *et al.* reported latencies of MEP for ECR muscles with 18.7 ± 1.6 ms from the unaffected side and 20.9 ± 3.1 ms from the affected side for chronic patients [6].

Several factors were possibly associated with the prolonged conduction time from the lesional hemisphere, although the exact mechanism is still under debate. The phase synchronization between EEG and EMG activities depends on the availability of corticospinal pathways for the transmission of descending potentials. However, the lesion around the region of basal ganglia possibly resulted in discontinuity of partial

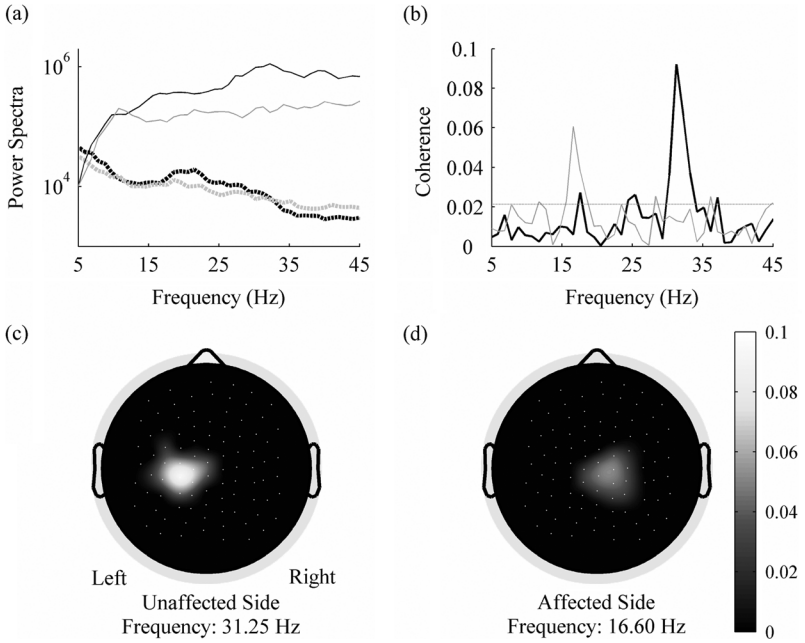

Fig. 4. Coherences and latencies analysis for subject 3. (a) Power spectra of EMG signals and EEG time series with highest significant coherence—channel 37 of the unaffected task (thin black line); channel 77 of the affected task (thin gray line); signal from the right ECR muscle of the unaffected task (black bold dotted line); signal from the left ECR muscle of the affected task (gray bold dotted line). The spectra were shifted vertically for clarity. (b) Highest significant coherence was found in EEG channel 37 at 31.25 Hz from the unaffected task (black line) and in channel 77 at 16.60 Hz from the affected task (gray line). (c) Topographic map of coherence at 31.25 Hz in the unaffected task. (d) Topographic map of coherence at 16.60 Hz in the affected task.

fast corticospinal tracts. The subsequent recruitment of slower conducting fibers could reduce the conduction velocity of the descending pathway [7]. Another factor to be considered was the temporal summation mechanism at the spinal level [32]. Since the discharge of motoneurons in the spinal cord relies on the summation of multiple descending volleys from the motor cortex, the reduction of available corticospinal tracts could result in the insufficient drive ability. The displacement of cortical representation area of muscles possibly reflected the local network reorganization and the unmasking or strengthening of survival corticospinal pathways. However, the increased threshold and depressed amplitude of MEP in the damaged hemisphere indicated the decreased excitatory ability of reorganized neural network in the ipsilesional M1 after recovery [3]–[7]. Consequently the compensation of descending drive ability by the reallocation in local neural network was limited. Hence, the prolonged conduction time observed in the current study possibly reflected the temporal compensation with successive potentials to recruit the motoneurons in the spinal cord.

TMS was a reliable method to measure the delay from the motor cortex to the muscles. However, MEP was absent for part of the stroke subjects and resulted in the unavailability of latency estimation [5], [6]. Therefore, the CMCoh provided an alternative way to measure the conduction time between the central rhythm and the electromyographic time series. Since these two technologies were based on distinct principles, the interpretations of the latencies were different. The result of TMS showed the conduction velocity of descending potentials using passive transcranial stimulation, while CMCoh relied on the steady and continuous synchronization between the cortical rhythm and electromyographic activities in an active mode. The latency measured by TMS reflected the basic property of the motor pathway while CMCoh showed a higher functional characteristic of the motor system, that is, the ability to promote the synchronization between upper and lower motoneurons to achieve optimal motor control [31].

B. Displacement of the Peak Coherence

Mima *et al.* first reported the topographical shift of CMCoh in the affected side for chronic stroke patients [16]. However, the localization of the maximum coherence could not be shown, which was possibly due to the low density EEG recording (56 channels). In the current study one 128-channel recording system was adopted to improve the spatial resolution of EEG signals. The electrodes projection optimization algorithm based on individual anatomical landmarkers, spherical surface laplacian and a mapping technique similar to the other TMS studies [3], [4] were applied to calculate the spatial coordinates of maximum coherence. Since the most significant CMCoh was always found in the precentral gyrus, the localization could be treated as a rough estimation of the muscles representation area after the cerebral reorganization.

Neuroimaging studies with fMRI, PET, and TMS have reported the displacement related to the brain plasticity after stroke [1]–[5]. The mechanisms that result in such shift may include the reallocation of the local network around the lesion in M1 and the recruitment of adjacent nonprimary motor cortex with direct cortical spinal tract (CST) projection, like the premotor cortex (PMC) and postcentral gyrus. Using a mapping technique, Byrnes *et al.* showed that the interhemispheric difference for MEP "hot spot" of APB muscles was within 2 mm for both medial–lateral and anterior–posterior directions with normal subjects [4]. And the upper limits for the difference were 3 mm in the medial–lateral axis and 9 mm

in the anterior–posterior axis. In the current study the mean displacement of interhemispheric maximum coherence was 14 mm in the interaural direction. The shifts showed consistent displacement towards the vertex except one subject (subject 5). Hence the cerebral reorganization of subjects in the current study possibly benefit from the recruitment of adjacent brain areas within the primary motor cortex except one subject (subject 6). The medial shift could denote a cortical reorganization towards the corticospinal tracts which innervate the proximal muscles. Most subjects showed a relatively small displacement in the nasion–inion direction. The shift could be rather the reallocation in local primary motor cortex than the recruitment of nonprimary motor area like the PMC or postcentral area. Nevertheless, the large posterior displacement of subject 6 possibly implied the recruitment of a neural network in postcentral gyrus with direct corticospinal fibers.

C. Decreased Coherence in the Affected Side

A significant difference of peak coherence value between the unaffected side and affected side was confirmed in the chronic stroke patients (see Table II) [16], and several factors possibly contribute to such observation. First of all, the impairment in the region of basal ganglia possibly led to the discontinuity of partial descending pathways. The neural activities via the pyramidal tracts were significantly reduced following brain injury and led to the decorrelation of the presynaptic and postsynaptic activities, which weaken the cortical-spinal synaptic connections. Although the displacement of CMCoh indicated that the wrist function was possibly recovered by the compensation of local network adaptation through existing CST, such compensation was less efficient than original pathways and possibly resulted in the lower drive ability of spinal motoneurons. Second, the properties of the motor units (MU) could also change as the result of damage to the CNS. This was confirmed by a firing pattern study of MU after stroke [33]. The neuromuscular disorders resulted in an increase in MU discharge variability and a decrease of the firing rate.

The CMCoh could be interpreted as the synchronized oscillatory between cortexes and spinal motoneurons to achieve optimal motor control [31]. This was especially important when executing sustaining accurate control tasks which need more concentration and effort. Therefore, the significant reduction of CMCoh in the lesional hemisphere could also be interpreted as the macroscopic depression of movement control in the affected side.

The uncrossed CST occupied about 10%–15% of total pathway originated from M1 in human beings although the exact proportion was unknown, and these pathways at least in principle could contribute to the motor recovery after stroke. However, no subject showed a significant coherence peak in the contralesional side in the current study, which implied the absence of contribution of the unaffected hemisphere to the movement control in CMCoh. This could be explained by the fact that the functional role for the ipsilateral hemisphere only showed in patients who did not make a good functional recovery [34].

D. Peak Frequency of CMCoh

The frequency of CMCoh reflected the preferred firing rates of MU under a specific condition, e.g., the force level for steady isometric control. Several factors were associated with the frequency of CMCoh, like the rhythmic activities in the motor cortex, the intrinsic properties of MU, and the force level of contraction [8], [28]. Although the peak frequency was found to increase as the magnitude of contraction force was raised [28], the particular value under a certain condition was still a subject-specific parameter with great variance (see Table II). The range of peak frequencies in the affected side was still within the beta band and no statistical difference was found between the results from two task groups. Such observation was consistent with the experimental finding from normal subjects [8], [28] and implied that the motor system tended to synchronize in the beta band in the condition of weak contraction even after cerebral plasticity.

V. Conclusion

The present study showed that the conduction time from cortical rhythm to the peripheral oscillations was significantly prolonged for the affected side than the unaffected side after subcortical stroke. Such observation possibly resulted from the damage to the corticospinal pathways and the local neural network relocation after stroke with consideration to the significantly decreased coherence value and the interhemisphere asymmetries of peak coherence. Hence, CMCoh could enrich our understanding of the cerebral plasticity of the motor system after stroke.

Acknowledgment

The authors would like to thank X. Hu, P. Lin, and M. Pohja for their valuable suggestions. The authors would also like to thank the staff of the Applied Cognitive Neuroscience Laboratory of Hong Kong Polytechnic University.

References

[1] R. Pineiro, S. Pendlebury, H. Johansen-Berg, and P. M. Matthews, "Functional MRI detects posterior shifts in primary sensorimotor cortex activation after stroke: Evidence of local adaptive reorganization?," *Stroke*, vol. 32, no. 5, pp. 1134–1139, 2001.

[2] C. Calautti, F. Leroy, J. Y. Guincestre, and J. C. Baron, "Displacement of primary sensorimotor cortex activation after subcortical stroke: A longitudinal PET study with clinical correlation," *NeuroImage*, vol. 19, no. 4, pp. 1650–1654, 2003.

[3] G. W. Thickbroom, M. L. Byrnes, S. A. Archer, and F. L. Mastaglia, "Motor outcome after subcortical stroke correlates with the degree of cortical reorganization," *Clin. Neurophysiol.*, vol. 115, no. 9, pp. 2144–2150, 2004.

[4] M. L. Byrnes, G. W. Thickbroom, B. A. Phillips, and F. L. Mastaglia, "Long-term changes in motor cortical organisation after recovery from subcortical stroke," *Brain Res.*, vol. 889, pp. 278–287, 2001.

[5] T. Platz, S. van Kaick, L. Moller, S. Freund, T. Winter, and I.-H. Kim, "Impariment-oriented training and adaptive motor cortex reorganisation after stroke: A fTMS study," *J. Neurol.*, vol. 252, pp. 1363–1371, 2005.

[6] C. M. Stinear, P. A. Barber, P. R. Smale, J. P. Coxon, M. K. Fleming, and W. D. Byblow, "Functional potential in chronic stroke patients depends on corticospinal tract integrity," *Brain*, vol. 130, pp. 170–180, 2007.

[7] G. Pennisi, G. Alagona, G. Rapisarda, F. Nicoletti, E. Costanzo, R. Ferri, M. Malaguarnera, and R. Bella, "Transcranial magnetic stimulation after pure motor stroke," *Clin. Neurophysiol.*, vol. 113, pp. 1536–1543, 2002.

[8] T. Mima and M. Hallett, "Corticomuscular coherence: A review," *J. Clin. Neurophysiol.*, vol. 16, no. 6, pp. 501–511, 1999.

[9] C. Gerloff, C. Braun, M. Staudt, Y. L. Hegner, J. Dichgans, and I. Krageloh-Mann, "Coherent corticomuscular oscillations originate from primary motor cortex: Evidence from patients with early brain lesions," *Human Brain Mapp.*, vol. 27, no. 10, pp. 789–798, 2006.
[10] S. Salenius, K. Portin, M. Kajola, R. Salmelin, and R. Hari, "Cortical control of human motoneuron firing during isometric contraction," *J. Neurophsiol.*, vol. 77, no. 6, pp. 3401–3405, 1997.
[11] J. Raethjen, M. Lindemann, M. Dümpelmann, R. Wenzelburger, H. Stolze, G. Pfister, C. E. Elger, J. Timmer, and G. Deuschl, "Corticomuscular coherence in the 6–15 Hz band: Is the cortex involved in the generation of physiologic tremor?," *Exp. Brain Res.*, vol. 142, no. 1, pp. 32–40, 2002.
[12] S. Ohara, T. Nagamine, A. Ikeda, T. Kunieda, R. Matsumoto, W. Taki, N. Hashimoto, K. Baba, T. Mihara, S. Salenius, and H. Shibasaki, "Electrocorticogram-electromyogram coherence during isometric contraction of hand muscle in human," *Clin. Neurophysiol.*, vol. 111, no. 11, pp. 2014–2024, 2000.
[13] R. B. Govindan, J. Raethjen, F. Kopper, J. C. Claussen, and G. Deuschl, "Estimation of time delay by coherence analysis," *Physica A*, vol. 350, pp. 277–295, 2005.
[14] J. Gross, P. A. Tass, S. Salenius, R. Hari, H.-J. Freund, and A. Schnitzler, "Cortico-muscular synchronization during isometric muscle contraction in humans as revealed by magnetoencephalography," *J. Physiol.*, vol. 527, no. 3, pp. 623–631, 2000.
[15] M. Pohja, S. Salenius, and R. Hari, "Reproducibility of cortex-muscle coherence," *NeuroImage*, vol. 26, no. 3, pp. 764–770, 2005.
[16] T. Mima, K. Toma, B. Koshy, and M. Hallett, "Coherence between cortical and muscular activities after subcortical stroke," *Stroke*, vol. 32, no. 11, pp. 2597–2601, 2001.
[17] J. Raethjen, M. Lindemann, M. Dümpelmann, R. Wenzelburger, H. Stolze, G. Pfister, C. E. Elger, J. Timmer, and G. Deuschl, "Corticomuscular coherence in the 6–15 Hz band: Is the cortex involved in the generation of physiologic tremor?," *Exp. Brain Res.*, vol. 142, no. 1, pp. 32–40, 2002.
[18] J. N. Caviness, C. H. Adler, M. N. Sabbagh, D. J. Connor, J. L. Hernandez, and T. D. Lagerlund, "Abnormal corticomuscular coherence is associated with the small amplitude cortical myoclonus in Parkinson's disease," *Movement Disorders*, vol. 18, no. 10, pp. 1157–1162, 2003.
[19] R. C. Oldfield, "The assessment and analysis of handedness: The Edinburgh inventory," *Neuropsychologia*, vol. 9, no. 1, pp. 97–113, 1971.
[20] A. R. Fugl-Meyer, L. Jaasko, I. Leyman, S. Olsson, and S. Steglind, "The post-stroke hemiplegic patient. 1. a method for evaluation of physical performance," *Scand. J. Rehabil. Med.*, vol. 7, no. 1, pp. 13–31, 1975.
[21] F. Tecchio, C. Porcaro, F. Zappasodi, A. Pesenti, M. Ercolani, and P. M. Rossini, "Cortical short-term fatigue effects assessed via rhythmic brain-muscle coherence," *Exp. Brain Res.*, vol. 174, no. 1, pp. 144–151, 2006.
[22] F. Perrin, J. Pernier, O. Bertrand, and J. F. Echallier, "Spherical splines for scalp potential and current-density mapping," *Electroencephalogr. Clin. Neurophysiol.*, vol. 72, no. 2, pp. 184–187, 1989.
[23] F. Perrin, "Correction," *Electroencephalogr. Clin. Neurophysiol.*, vol. 76, no. 6, pp. 565–565, 1990.
[24] J. R. Rosenberg, A. M. Amjad, P. Breeze, D. R. Brillinger, and D. M. Halliday, "The fourier approach to the identification of functional coupling between neuronal spike trains," *Prog. Biophys. Mol. Biol.*, vol. 53, no. 1, pp. 1–31, 1989.
[25] A. Delorme and S. Makeig, "EEGLAB: An open source toolbox for analysis of single-trial EEG dynamics including independent component analysis," *J. Neurosci. Methods*, vol. 134, no. 1, pp. 9–21, 2004.
[26] D. Kaplan and L. Glass, *Understanding Nonlinear Dynamics*. New York: Springer-Verlag, 1995.
[27] J. Theiler, S. Eubank, A. Longtin, B. Galdrikian, and J. D. Farmer, "Testing for nonlinearity in time series: The method of surrogate data," *Physica D*, vol. 58, pp. 77–94, 1992.
[28] P. Brown, S. Salenius, J. C. Rothwell, and R. Hari, "Cortical correlate of the piper rhythm in humans," *J. Neurophysiol.*, vol. 80, pp. 2911–2917, 1998.
[29] T. Mima and M. Hallett, "Electroencephalographic analysis of corticomuscular coherence: Reference effect, volume conduction and generator mechanism," *Clin. Neurophysiol.*, vol. 110, no. 11, pp. 1892–1899, 1999.
[30] T. Mima, J. Steger, A. E. Schulman, C. Gerloff, and M. Hallett, "Electroencephalographic measurement of motor cortex control of muscle activity in humans," *Clin. Neurophysiol.*, vol. 111, no. 2, pp. 326–337, 2000.
[31] A. Schnitzler and J. Gross, "Normal and pathological oscillatory communication in the brain," *Nat. Rev. Neurosci.*, vol. 6, no. 4, pp. 285–296, 2005.
[32] K. Kaneko, S. Kawai, Y. Fuchigami, G. Shiraishi, and T. Ito, "Spinal cord potentials after transcranial magnetic stimulation during muscle contraction," *Muscle Nerve*, vol. 19, no. 5, pp. 659–661, 1996.
[33] C. K. Thomas, J. E. Butler, and I. Zijdewind, "Patterns of pathological firing in human motor units," *Adv. Exp. Med. Biol.*, vol. 508, pp. 237–244, 2002.
[34] D. J. Serrien, L. H. A. Strens, M. J. Cassidy, A. J. Thompson, and P. Brown, "Functional significance of the ipsilateral hemisphere during movement of the affected hand after stroke," *Exp. Neurol.*, vol. 190, no. 2, pp. 425–432, 2004.

Fei Meng was born in the Hebei province of China, in 1976. He received the B.E. and M.E. degrees in biomedical engineering from the Tsinghua University, Beijing, China, in 1999 and 2002, respectively.

His research interests include brain–computer interface (BCI), neural system modeling and signal processing and the rehabilitation of stroke.

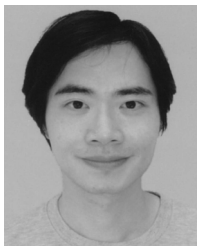

Kai-Yu Tong (SM'08) received the Ph.D. degree in bioengineering from the University of Strathclyde, Glasgow, U.K., in 1998.

He spent four months as a Research Fellow at Strathclyde University and participated in a joint project with the Spinal Cord Injury Unit, Southern General Hospital, Glasgow, U.K. He joined the Hong Kong Polytechnic University in 1999 and as an Associate Professor in the Department of Health Technology and Informatics, in 2008. His research interests include rehabilitation robot, the control of functional electrical stimulation for upper and lower extremity functions, sensor development, stroke rat model, and BCI training rehabilitation on persons after stroke.

Suk-Tak Chan received the Ph.D. degree in radiography (ultrasound) and the M.Sc. degree in information technology from The Hong Kong Polytechnic University, Kowloon, Hong Kong, in 2006 and 1999, respectively

She joined the Hong Kong Polytechnic University as Assistant Professor in 1997. She was a Research Fellow at the Massachusetts General Hospital, Harvard Medical School, Boston, in 2000. She specializes in the structural and functional MR neuroimaging techniques and analysis. She is also interested in MR sequence development and the cognitive studies using magnetoencephalography.

Wan-Wa Wong received the B.Sc. degree in biomedical engineering, in 2007, from the Hong Kong Polytechnic University, Kowloon, Hong Kong, where she is currently working towards the Ph.D. degree in biomedical engineering.

Her research interests include structural and functional magnetic resonance imaging and electroencephalography studies of motor imagery in persons after chronic stroke.

Ka-Him Lui received the B.Sc. degree in biomedical engineering from the Hong Kong Polytechnic University, Kowloon, Hong Kong, in 2007.

His current research interest is related to brain–computer interface and function electrical stimulation for stroke patients.

Kwok-Wing Tang has been a Fellow of the Royal College of Radiologists since 1992. He joined the Department of Radiology and Imaging at the Queen Elizabeth Hospital in 1989 and is now a Consultant Radiologist in the same department. He specializes in neuroradiology and neurointervention.

Xiaorong Gao was born in Beijing, China, in 1963. He received the B.S. degree in biomedical engineering from Zhejiang University, Zhejiang, China, in 1986, the M.S. degree in biomedical engineering from Peking Union Medical College, Beijing, China, in 1989, and the Ph.D. degree in biomedical engineering from Tsinghua University, Beijing, China, in 1992.

He is currently a Professor of the Department of Biomedical Engineering, Tsinghua University. His current research interests are biomedical signal processing and medical instrumentation, especially the research of brain–computer interface.

Shangkai Gao (SM'94–F'07) graduated from the Department of Electrical Engineering and received the M.E. degree in biomedical engineering from Tsinghua University, Beijing, China, in 1970 and 1982, respectively.

She is currently a Professor of the Department of Biomedical Engineering, Tsinghua University. Her research interests include biomedical signal processing and medical ultrasound.

Prof. Gao is an Associate Editor of IEEE TRANSACTIONS ON BIOMEDICAL ENGINEERING and IEEE TRANSACTIONS ON NEURAL SYSTEM AND REHABILITATION ENGINEERING.